Invited Paper

Molecular beam epitaxial growth and characterization of (001) $Hg_{1-x}Cd_xTe$-HgTe superlattices

C.R. Becker, V. Latussek, H. Heinke, M.M. Regnet, F.Goschenhofer,
S. Einfeldt, L. He[a] E. Bangert, M.M. Kraus, and G. Landwehr
Physikalisches Institut der Universität Würzburg, Am Hubland, 97074 Würzburg, Germany

ABSTRACT

The molecular beam epitaxially growth of (001) $Hg_{1-x}Cd_xTe$-HgTe superlattices has been systematically investigated. The well width as well as the period were determined directly by X-ray diffraction. This was accomplished for the well width by exploiting the high reflectivity from HgTe and the low reflectivity from CdTe for the (002) Bragg reflection. Knowing the well and barrier thicknesses we have been able to set an upper limit on the average composition of the barriers, $\bar{x}_b$, by annealing the superlattice and then measuring the composition of the resulting alloy. $\bar{x}_b$ was shown to decrease exponentially with decreasing barrier width. $\bar{x}_b$ is appreciably smaller in narrow barriers due to the increased significance of interdiffusion in the $Hg_{1-x}Cd_xTe$/HgTe interface in narrow barriers.

The experimentally determined optical absorption coefficient for these superlattices is compared with theoretical calculations. The absorption coefficient was determined from transmission and reflection spectra at 300, 77 and 5 K. Using the thickness and composition of the barriers and wells, and an interface width due to interdiffusion, the complex refractive index is calculated and compared with the experimental absorption coefficient. The envelope function method based on an 8×8 second order $\mathbf{k} \cdot \mathbf{p}$ band model was used to calculate the superlattice states. These results, when inserted into Kubo's formula, yield the dynamic conductivity for interband transitions. The experimental and theoretical values for the absorption coefficient using no adjustable parameters are in good agreement for most of the investigated superlattices. Furthermore the agreement for the higher energetic interband transitions is much worse if values for the barrier composition, which are appreciably different than the experimentally determined values, are used.

The infrared photoluminescence was investigated at temperatures from 4.2 to 300 K. Pronounced photoluminescence was observed for all superlattices in this temperature range.

I. INTRODUCTION

Schulman and McGill[1] proposed in 1979 that the CdTe-HgTe superlattice would be a useful material for a number of infrared optoelectronic devices. They predicted that the band gap of the superlattice should be adjustable from 0 to 1.6 eV depending on the CdTe and HgTe layer thicknesses and they suggested that the growth could be carried out by molecular beam epitaxy (MBE). This was first accomplished by Faurie *et al.* in 1982.[2] Thereafter numerous publications have dealt with the novel electrical and optical properties of these structures, which have been reviewed by Faurie,[3] McGill *et al.*,[4] Meyer *et al.*[5] and others.

The CdTe-HgTe superlattice has potential advantages in infrared applications compared to the alloy. For example, better control over the band gap of narrow gap superlattices has been predicted.[6,7] The band gap is controlled primarily by the well thickness and to a lesser extent by the barrier thickness. It increases from approximately 10 to 200 meV when the well width is reduced from 100 to 30 Å. In contrast the band gap of the alloy depends on its composition which has to be progressively better controlled as the band gap goes to zero. The band gap of a superlattice is a smooth, slowly varying function of the layer thicknesses and hence arguably easier to control. However the barrier normally consists of $Hg_{1-x}Cd_xTe$ and not CdTe because the Hg flux is left on during growth and both Hg and Cd compete for cation sites. The composition of the well and the barrier influences the height of the potential barrier between the two and hence the band gap. Their x values are not readily accessible but should depend primarily on their initial values, i.e. on the growth parameters, and in the case of narrow layers on subsequent interdiffusion. Kim *et al.*[8] have shown that interdiffusion is two orders of magnitude larger near the surface when compared to a depth of 7000 Å or more. Therefore interdiffusion should depend primarily on how long a particular layer spends near the surface which is constant with the exception of the superlattice periods grown last.

The superlattice period is readily accessible by x-ray diffraction experiments, however the well and barrier thicknesses and their compositions are not so easily determined. Historically well and barrier thicknesses have been inferred

0-8194-1270-8/93/$6.00

from the growth parameters or measured by transmission electron microscopy (TEM).[9] We have been able to determine the well thickness and hence that of the barrier by means of high resolution x-ray diffraction.[10,11] This is done by taking advantage of the large HgTe structure factor compared to that of CdTe for the (002) Bragg reflection. The well thickness as determined by this method has been corroborated by (TEM) for a superlattice with an extremely short period of 31.4 Å.

The composition of the well and barrier can not be determined directly except possibly by a destructive method such as chemical mapping[8] which utilizes TEM. In this investigation we have estimated the composition of the initial barrier material by means of transmission and reflection measurements on thick test layers of (001) $Hg_{1-x}Cd_xTe$ grown under identical conditions with the exception of the presence of the HgTe wells. Knowing the well and barrier thicknesses we have been able to set an upper limit on the actual composition of the barriers by annealing several superlattices and then measuring the composition of the resulting alloy.

A large number of band structure calculations for the $Hg_{1-x}Cd_xTe$-HgTe superlattice have been published during the last decade.[5,12-14] Ram-Moham *et al.*[12] employed the envelope function method and developed a transfer matrix procedure to calculate the superlattice states. He accounted for the full 8×8 Kane hamiltonian including all second order terms representing the far-band contributions, but did not apply his results to a calculation of the optical constants. On the other hand N.F. Johnson *et al.*[13] applied a slightly different version of the envelope function method, and deduced optical constants from his superlattice energies and eigenfunctions. But in his approach he used a simplified band model, which omits all the second order far-band contributions, with the exception of a finite heavy hole mass. In order to overcome these shortcomings, we have combined the essential aspects of both approaches.[15] This enables us to calculate the optical constants based on a realistic band structure model, which includes all second order higher band contributions. This should be a sound basis for a realistic comparison between theory and experiment.

II. EXPERIMENTAL AND THEORETICAL DETAILS

A. Growth

Epitaxial growth was carried out in a four chamber RIBER 2300, molecular beam epitaxial (MBE) system which has been modified to permit the growth of Hg based materials. The vacuum in the growth chamber is better than 6×10^{-10} Torr when no Hg has recently been admitted. Three MBE cells were employed, two of which were commerical cells and which contained high purity CdTe and Te. The third cell is a self designed stainless steel cell for Hg which can be refilled without breaking the vacuum. The flux of the latter cell is stable to within ± 1.5 and ± 3 % over a period of 2 and 30 hours, respectively. The CdTe and Te fluxes depend upon how long their respective shutters have been closed and/or open. This is discussed in more detail elsewhere.[11] The steady state values for CdTe, Te and Hg were 3×10^{-7}, 6×10^{-7} and 2.8×10^{-4} Torr, respectively. In this article pressure is loosely referred to as flux. This Hg flux is roughly 2.5 times larger than the minimum flux necessary to maintain epitaxial growth of HgTe.

The $Hg_{1-x}Cd_xTe$-HgTe superlattices were grown on (001) $Cd_{0.96}Zn_{0.04}Te$ and CdTe substrates which had been degreased, chemo-mechanically polished for several minutes in a weak solution of bromine in methanol and then rinsed in methanol. Two substrates which were chemo-mechanically polished by the manufacturer (epi-ready) were merely degreased, i.e. Q424 and Q426. Immediately prior to mounting the $5 \times 10 \times 1$ mm substrates on a molybdenum holder with a solution of graphite in isopropanol and loading into the MBE system, they were rinsed in de-ionized water, briefly dipped in hydrochloric acid and then rinsed in de-ionized water so as to remove all of the original oxide and carbon from the substrate surface.[16] We have found that the newly formed oxide as a result of this previous step, is much more easily evaporated from the surface.[17] This is accomplished by heating the substrates at temperatures up to about $320°C$ while monitoring the substrate surface by reflection high energy electron diffraction (RHEED) as described elsewhere.[18] The substrate temperature was measured with an accuracy of $\pm 2°C$ by means of a thermocouple which was in physical contact with a molybdenum substrate holder. The thermocouple was carefully calibrated at the melting points of indium and tin.

Before the superlattice was grown, a thin CdTe buffer was grown on the (001) $Cd_{0.96}Zn_{0.04}Te$ or CdTe substrate at $270°C$ until the reflection high electron energy diffraction (RHEED) pattern indicated that the surface was smooth by the presence of short streaks. The thickness of this buffer was between 30 and 1000 Å. This surface was characterized by a (2×1) half order reconstruction in the $[0\bar{1}1]$ azimuth. We use the convention of refering to the direction of the incident electrons when refering to reconstruction in a particular azimuth. The superlattice was then grown at $180°C$.

B. X-ray diffraction details and theory

We have used a high resolution five crystal x-ray diffractometer to determine accurate values for the well thickness, the average superlattice period and the deviation from this average in the superlattice. The Cu $K\alpha_1$ radiation was resolved by means of the Ge (220) Bragg reflection in a four crystal monochromator. The reasons for a measurable (002) Bragg reflection for the zinc blende structure as opposed to the diamond structure where it is forbidden is discussed by Möller *et al.*.[10] The rather large (002) Bragg reflection in these superlattices is caused primarily by the HgTe well; the structure factor for the (002) Bragg reflection is much larger for HgTe than for CdTe.[10] To our knowledge this behavior, the large difference in the size of the structure factor between HgTe and CdTe, is unique to this system and perhaps to related Hg containing superlattices. This is due to the relatively large size of the Hg atom with its large number of electrons. In fact the structure factor goes to zero for $Hg_{1-x}Cd_xTe$ with an x value of about 0.88. Thus an observable envelope of the superlattice satellites is due to the slit function corresponding to the HgTe layers. From the angular separation of the first order zero points of this envelope, $\Delta\omega_{Z.P.}$, we can calculate the average thickness of the HgTe well, $\bar{t}_w$, with an accuracy of $\geq \pm 3$ Å, which depends on the number of satellites and the position of the first order zero points, $\Delta\omega_{Z.P.}$, relative to the satellites. Similarily the average superlattice period, $\bar{t}_P$, can be determined from the angular separation of the superlattice satellites, $\Delta\omega_P$. From the increased broadening of the higher order satellites, $\delta\omega_{\text{Sat.}}$, for the (004) reflection, the deviation of the superlattice period from its average value throughout the structure can be obtained. Here we have used the following equations:[19]

$$\bar{t}_P = \frac{\lambda|\gamma_H|}{\Delta\omega_P \sin(2\theta_B)} \tag{1}$$

$$\frac{\delta t_P}{\bar{t}_P} = \frac{\delta\omega_{\text{Sat.}}\bar{t}_P \sin(2\theta_B)}{\lambda|\gamma_H|} \tag{2}$$

$$\bar{t}_w = \frac{2\cdot\lambda|\gamma_H|}{\Delta\omega_{Z.P.}\sin(2\theta_B)} \tag{3}$$

where λ is the wavelength of the reflected x-rays, θ_B is the Bragg angle for the substrate, γ_H is $\vec{k}_H \times \vec{n}$, $\vec{k}_H$ is the scattered unit wave vector and $\vec{n}$ is the unit vector normal to the surface.

C. Composition of wells and barriers

In order to determine the composition of our barriers, we have grown alloys with the same CdTe and Hg fluxes and at the same temperature used for the superlattice. In addition we have grown alloys with periodic growth stops of the same duration as that required for the growth of the HgTe well. In other words the growth conditions including the opening and closing of the Te and CdTe shutters were identical, with the exception of no Te flux. We determined the composition of the alloys grown by both of these methods from the E_0[20] and E_1 (L6-L4,5)[21,22] energy gaps by means of transmission and reflection measurements, respectively, to be 0.68 ±0.02. However one condition, the presence of the HgTe wells, is not the same and interdiffusion in these short period superlattices must be taken into consideration.

In order to set an upper limit on the average barrier composition, $\bar{x}_b$, annealing experiments were carried out on several superlattices at 240 to 250°C for 24 hours. The superlattice was placed in a quartz ampoule together with either a drop of Hg which could not come into contact with the superlattice or with 400 mbar of 99.999% pure Ar gas. In the latter case, the superlattice surface was held in contact with a clean CdTe substrate by means of a weak tantalum spring on a piece of molybdenum.

D. Optical absorption coefficient

1. Experiment

Optical transmission and reflection measurements were carried out in the middle and near infrared with a Fourier transform spectrometer, IFS88, from Bruker Instruments Inc. A deuterated triglycine sulfate detector was employed rather than a liquid nitrogen cooled detector, *e.g.* $Hg_{1-x}Cd_xTe$, because of its better linearity. The aperature was kept as small as possible for the same reason, i.e. a diameter of 2 to 3 mm. The absorpion coefficient was

determined by fitting the experimental transmission and reflection spectra to a theoretical description of the multilayer system using the standard matrix procedure. Minimizing the difference between experimental and theoretical values of merely the transmission at a constant index of refraction resulted in the same absorption coefficient within experimental uncertainity. Therefore, in most cases this procedure was carried out for only the transmission using an appropriate constant refractive index.

2. Theory

The envelope function method of Bangert *et al.*[15] was employed which differs formally from previous ones.[12,13] It was conceived in such a way as to yield a large number of superlattice energies, wave functions and dipole matrix elements which are needed for the calculation of the optical absorption. The bands of both bulk HgTe and CdTe are described by Kane's four-band model (8×8 $\mathbf{k} \cdot \mathbf{p}$) including second order far-band contributions, but neglecting the small anisotropy of the valence bands. The effects of strain due to lattice mismatch were also taken into consideration.[14] The numerical values for the band parameters (E_g, Δ, γ_1, γ_2, γ_3, F and E_p) were deduced from measurements on bulk HgTe and $Hg_{1-x}Cd_xTe$ by Weiler.[23] The valence band offset between HgTe and CdTe was taken to be 350 meV which is the generally accepted value.[5] The valence band offset for $Hg_{1-x}Cd_xTe$ was then assumed to vary linearly with x.[24] The thickness of the layers, and the superlattice period were determined by means of x-ray diffraction as discussed above. The composition of the barrier was taken to be that of alloys grown under the same conditions , i.e. 0.68 ± 0.02, and not the average x value in the barrier. This value for the alloy was used in conjunction with the interface width due to interdiffusion of the interface according to Kim *et al.*[8] which was integrated into the theory.

The real and imaginary components ($n(\omega)$ and $k(\omega)$) of the complex refractive index are obtained from

$$N^2(\omega) = (n(\omega) + ik(\omega))^2 = \varepsilon_L(\omega) + i\frac{\sigma(\omega)}{\omega\epsilon_0} \tag{4}$$

where $\varepsilon_L(\omega)$ is the lattice contribution and $\sigma(\omega)$ the dynamic conductivity. $\sigma(\omega)$ is determined by making use of Kubo's formula[15] which employes the superlattice energies, wave functions and dipole matrix elements mentioned above. It should be emphasized that no adjustable parameters are included in this theory.

III. RESULTS AND DISCUSSION

A. Photoluminescence measurements

Fourier transform infrared luminescence spectra of some of these superlattices have been published elsewhere.[11,25] The photoluminescence spectra of almost all of the superlattices in this investigation consist of one nearly symmetric line. The full width at half maximum of this line lies between 16 and 60 meV at 4.2 K and between 52 and 113 meV at 300 K. This attests to the good quality of these superlattices.

B. X-ray diffraction measurements

A smoothed rocking curve of the (002) reflection for the superlattice Q230 and the slit function used for the HgTe well thickness determination are shown in Fig.1 as the full and dotted lines, respectively. The large number of satellites which is typical of most of the investigated superlattices, is an indication of the high structural quality of these superlattices. The period, well and barrier thicknesses of all the superlattices investigated are listed in Table 1. The variation of these periods from their average values, according to Eq. 2, is less than 10 % and in most cases less than 5 %. This is also an indication of the good uniformity of these superlattices. The experimental uncertainity in the period and the HgTe well thickness is ± 0.5 and $\geq \pm 3$ Å, respectively.

Two of four extremely short period superlattices, Q250a and Q250c, which were grown simultaneously, have been investigated by x-ray diffraction in greater detail.[11] The rocking curve for the (002) Bragg reflection and a simulation of Q250a are shown in Fig.2. The simulation was calculated using a concentration profile across the $Hg_{1-x}Cd_xTe$-HgTe interface with the same width and shape as the interface according to Kim *et al.*[8] If an abrupt interface was employed then the simulated intensities of the satellites were much larger, *e.g.* the second order satellites were one

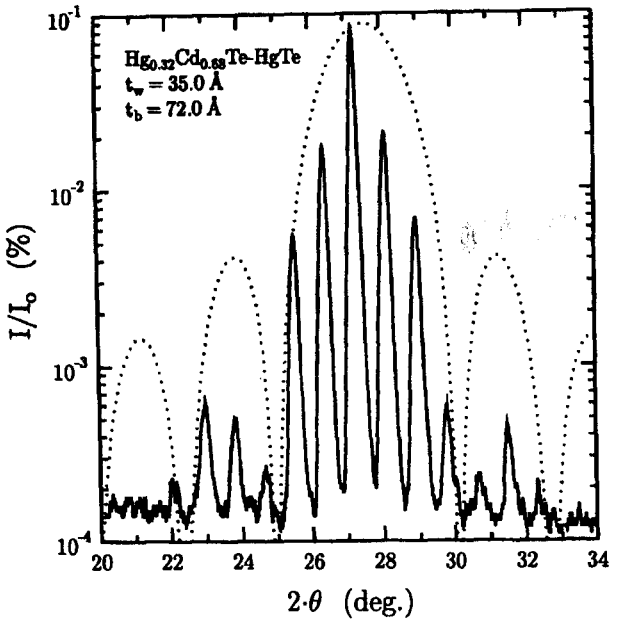

FIG. 1. X-ray rocking curve for the (002) Bragg reflection from the $Hg_{0.32}Cd_{0.68}Te$-HgTe superlattice Q230. The full line represents the experimental data and the dotted line is the envelope of the superlattice satellites which is due to the slit function corresponding to the HgTe layers. The large number of satellites is an indication of the excellent structural quality of the superlattice.

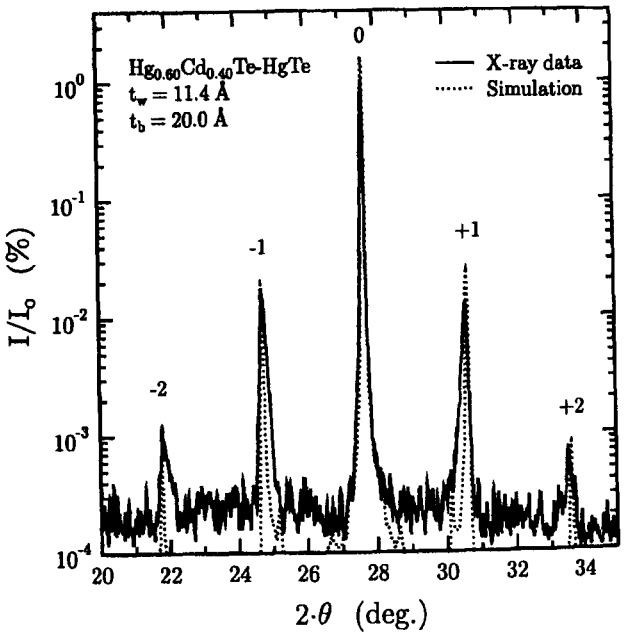

FIG. 2. X-ray rocking curve for the (002) Bragg reflection from the $Hg_{0.60}Cd_{0.40}Te$-HgTe superlattice Q250a. The full line with random noise represents the experimental data and the dotted line is a simulation of the data.

to two orders of magnitude larger. Furthermore, if an interface with approximately twice the width of the published interface was used, then the second order satellites were no longer discernible. Thus according to these simulations, the concentration profile across the $Hg_{1-x}Cd_xTe$-HgTe interface in these superlattices is similar to that of the interface according to Kim *et al.*[8]

The rocking curve of the (004) Bragg reflection for one of the superlattices which was grown on an epi-ready $Cd_{0.96}Zn_{0.04}Te$ substrate is shown in Fig. 3. The full width at half maximum (FWHM) is 22 and 19 arc seconds for the main superlattice peak and the substrate, respectively. The value for the superlattice, which is only slightly larger than that of the substrate, compares favorably with the best published values for a $Hg_{1-x}Cd_xTe$- HgTe superlattice, *e.g.* Myers *et al.*,[26] as well as with values for the best GaAs-$Al_xGa_{1-x}As$ superlattices. The (002) rocking curve for this superlattice is displayed in Fig. 4. The negative even order satellites, i.e. -2, -4 and -6, are completely missing due to the slit function which corresponds to the HgTe well thickness. The fact that the +2 and +4 satellites are still present, albeit appreciably weaker, can be explained by a slight difference in the lattice constant of the superlattice and that of the well; the position of the principal superlattice peak is determined by the lattice constant of the superlattice, whereas the position of the slit function is given by the lattice constant of the scattering material, i.e. the well. A simulation of the (002) rocking curve for Q426 using a concentration profile with the same width and shape as the experimentally determined profile mentioned above,[8] resulted in a better fit between the simulated and experimental satellite intensities than a simulation utilizing an abrupt interface. This concentration profile is shown in Fig.5.

C. Composition of wells and barriers

Prior to approximately 1986 the composition of the well and barrier material in $Hg_{1-x}Cd_xTe$-HgTe superlattices was assumed to be HgTe and CdTe, respectively. In 1987 Reno *et al.*[27] determined the x value of a thin layer, i.e.

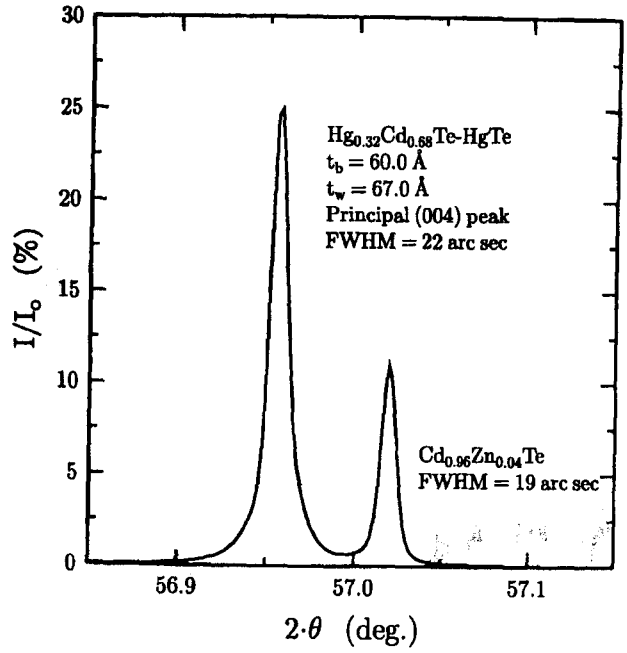

FIG. 3. X-ray rocking curve for the (004) Bragg reflection from the $Hg_{0.32}Cd_{0.68}Te$-HgTe superlattice Q426.

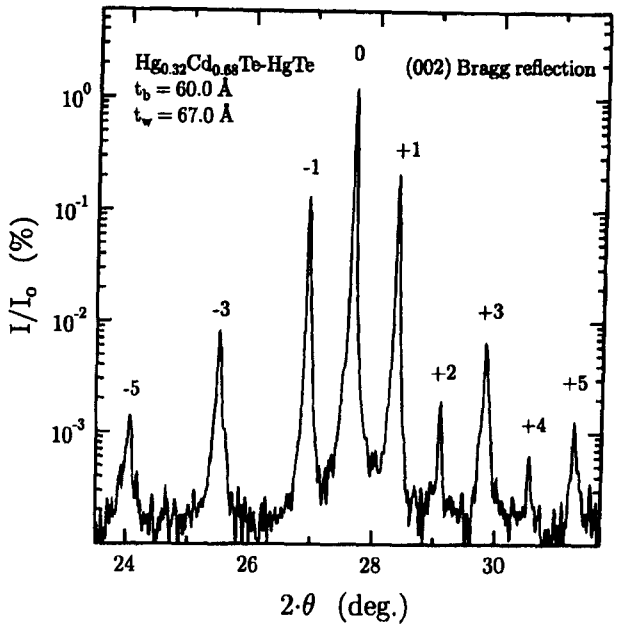

FIG. 4. X-ray rocking curve for the (002) Bragg reflection from the $Hg_{0.32}Cd_{0.68}Te$-HgTe superlattice Q426.

150-170 Å of (001) $Hg_{1-x}Cd_xTe$ barrier material grown at $185°C$ to be 0.85 by x-ray photoelectron spectroscopy. Due to absorption of the photo-emitted electrons, this is the x value for approximately 50 Å of the layer near the surface. Later Schulman *et al.*[9] determined the x value of a test layer of (001) $Hg_{1-x}Cd_xTe$ grown at $175°C$ to be 0.85. Most of the recent literature either assumes this x value to be correct, independent of the substrate temperature and the other growth parameters, or does not mention how the x value is determined. A recent exception is the work of Monterrat *et al.*[28] which reports an x value of approximately 0.70 for barrier material in (001) single and multiple quantum wells grown at $180°C$.

As mentioned above, the composition of alloys grown with the same growth parameters as those used for our barrier material was determined to be 0.68 ± 0.02. We found that MBE growth with the same growth conditions as described above but with illumination of the substrate with an Ar ion laser, resulted in an x value of 0.85. Wu *et al.*[18] have shown that illumination with an Ar ion laser as well as irradiation with the high energy electrons used in their RHEED oberservations, i.e. 10 keV, significantly reduces the desorption time for excess Te from a Te stabilized CdTe surface. Because the x value of $Hg_{1-x}Cd_xTe$ is governed primarily by the substrate temperature and the CdTe to Te flux ratio,[22] an enhanced desorption of Te from $Hg_{1-x}Cd_xTe$ would result in a larger x value. This is consistent with our observations from RHEED oscillations that the growth rate for $Hg_{0.32}Cd_{0.68}Te$ and HgTe decreases with increasing high energy electron intensity, i.e. an electron current of 200 μA results in a 10% reduction in growth rate. A larger x could also be caused by an enhanced Hg desorption, however this does not seem probable; the magnitude of the Hg flux which is approximately 2.5 times larger than that necessary to maintain epitaxial growth does not significantly influence either the x value of $Hg_{1-x}Cd_xTe$ or the growth rate.[22]

In order to determine the composition of the barrier in these superlattices, four superlattices were annealed at $250°C$ for 24 hours in an Ar atmosphere and one in a Hg atmosphere as described above. Both of these methods should be effective in reducing or preventing the diffusion of Hg out of the superlattice near the surface. If Hg does diffuse out of the superlattice, then the x value of the resulting alloy and the calculated value for $\bar{x}_b$ would be upper limits. Diffusion of Hg into the superlattice under an Hg atmosphere is possible, which would lower the x value near the surface.

The x value of one of the resulting alloys was determined from reflection measurements of the E_1 gap to be $0.48 \pm .01$. The corresponding x value from transmission measurements of the E_0 gap is somewhat higher, i.e. 0.52. Furthermore the discrepency between the E_0 and the E_1 gap increases with decreasing superlattice thickness. This is an indication

TABLE I. The number of periods, the period (Å), thickness(Å) and average Cd concentration of both the well and barrier for the investigated superlattices. Both measured values of the Cd concentration for the barriers, $\bar{x}_b$, and empirical values for $\bar{x}_b$ and $\bar{x}_w$, which were calculated by using the Cd concentration profile according to Ref.8, are included. Experimental and theoretical values for the energy gap, i.e. $HH_1 \rightarrow C_1$ for the investigated superlattices, are listed for a number of the superlattices at 5 and 300 K.

	Periods	$\bar{l}_P$	$\bar{l}_w$	$\bar{l}_b$	$\bar{x}_w$	$\bar{x}_b$	$\bar{x}_b$	Energy gap; $HH_1 \rightarrow C_1$ (meV)			
								theoretical		experimental	
		± 0.5	± 3	∓ 3	empirical		experimental	5 K	300 K	5 K	300 K
Q250	900	31.4	11.4	20.0	0.04	0.44	0.36 ± 0.05	118 ± 50^a	216 ± 54^a	120	200
Q211	100	47.0	16.0	31.0	0.03	0.53	0.50 ± 0.05				
Q178	90	54.1	30.6	23.5	0.02	0.48					
Q218	100	64.9	32.2	32.7	0.02	0.54	0.55 ± 0.05	178 ± 39	260 ± 35	210	300
Q168	180	67.4	29.6	37.8	0.02	0.56		208 ± 41	286 ± 36	155	300
Q247	100	82.5	31.4	51.1	0.02	0.59					
Q215	100	120.8	30.7	90.1	0.02	0.64		251 ± 32	329 ± 29	250	305
Q174	90	121.0	30.3	90.7	0.02	0.64	0.64 ± 0.03	242 ± 32	320 ± 30	210	300
Q167	140	87.0	35.1	51.9	0.01	0.59		177 ± 29	259 ± 26	160	260
Q230	100	107.0	35.0	72.0	0.01	0.62		204 ± 26	285 ± 25	210	280
Q424	120	110.7	34.7	76.0	0.01	0.63		195 ± 27	276 ± 25	180	272
Q214	100	76.0	40.0	36.0	0.01	0.55		125 ± 28	211 ± 25	190	240
Q200	100	77.1	38.4	38.7	0.01	0.56		143 ± 28	228 ± 26	174	245
Q195	100	82.0	38.7	43.3	0.01	0.58		150 ± 26	234 ± 25	160	235
Q163	100	89.0	40.0	49.0	0.01	0.59	0.60 ± 0.03	136 ± 24	220 ± 23		225
Q204	20	96.8	38.9	56.9	0.01	0.61		164 ± 23	247 ± 22	140	220
Q164	80	116.1	43.0	73.1	0.01	0.62		137 ± 18	220 ± 18		211
Q171	90	129.1	43.5	85.6	0.01	0.63					
Q162	100	80.0	47.9	32.1	0.01	0.54		55 ± 24	146 ± 22		176
Q426	110	127.0	67.0	60.0	0.01	0.63		53 ± 10	130 ± 10	27^b	120
Q165	100	106.0	63.0	43.0	0.01	0.55		25 ± 2	112 ± 12		110

[a]These results for the energy gap were calculated using $x_o = 0.40$ instead of $x_o = 0.68$ which was employed for all of the other energy gaps listed in this table.
[b]This energy gap was determined by means of magnetoabsorption measurements

that diffusion between the CdTe substrate and the $Hg_{1-x}Cd_xTe$ alloy is responsible for this discrepency. Reflection measurements should be less sensitive to changes in x due to diffusion near the substrate/alloy interface. Therefore x values as determined from reflection measurements of the E_1 gap are used in the following with one exception. The exception is the superlattice which was annealed in an Hg atmosphere and could consequently have a lower x value near the surface. In view of the uncertainity in this case, an average of the two x values (i.e. 0.24 and 0.22 for the E_0 and E_1 gap, respectively) is employed.

If all of the CdTe is in the barrier whose width is 91 ± 3 Å, then $\bar{x}_b$ is $0.64 \pm .03$. Obviously, this is an upper limit for $\bar{x}_b$ due to the assumption that all of the CdTe is in the barrier. Interdiffusion between the well and the barrier becomes more prominent as the well and barrier become thinner. The $\bar{x}_b$ upper limit for these samples are plotted as a function of the barrier width in Fig.6 and are listed in Table 1. As can be seen, $\bar{x}_b$ is appreciably lower for narrower barriers.

As mentioned above, Kim *et al.*[8] have experimentally determined the concentration profile in a similar superlattice which was also grown at 180°C. By assuming that the width and shape of the interfaces in this investigation are the same (see Fig.5), as suggested by the satellite intensity simulations which were discussed in the section on x-ray

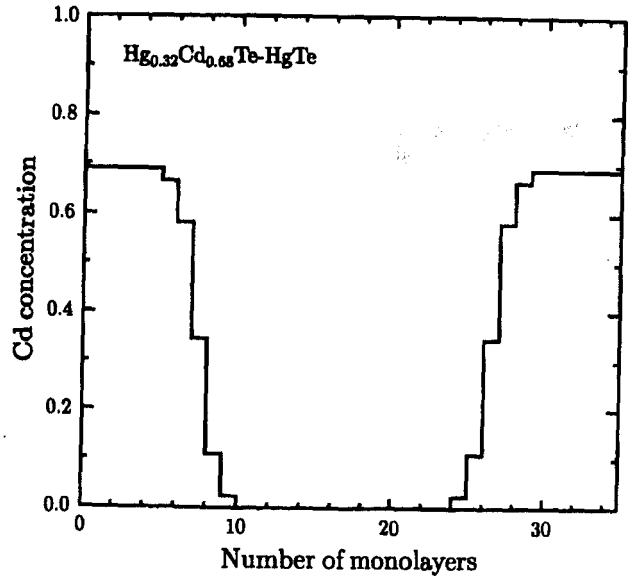

FIG. 5. Cd concentration profile used in the x-ray simulation and in the empirical determination of the average Cd barrier concentration, $\bar{x}_b$, for Q426. The width and shape of the $Hg_{0.32}Cd_{0.68}Te$-HgTe interface is the same as the experimental width and shape according to Ref.8.

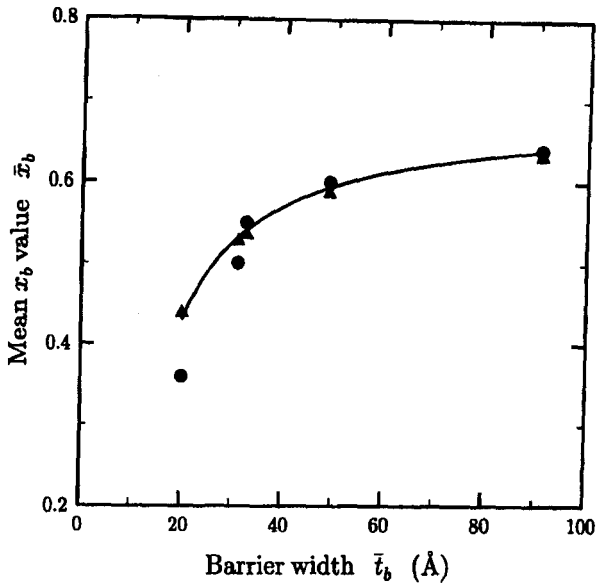

FIG. 6. $\bar{x}_b$ as a function of the barrier width is shown as filled circles. The filled triangles represent values which have been calculated using the Cd concentration profile published in Ref.8. The curve is a least square fit of an exponential function to the calculated data, see Eq. 4.

diffraction, we have calculated values for $\bar{x}_b$, which are displayed as triangles in Fig.6. The boundaries of the barriers were consistently chosen to occur at an x value of 0.16 so as to ensure a better fit to the experimental data for the wider barriers. The fit of these calculated values to the experimental data is reasonable with a slightly worse fit for narrow barriers. This is to be expected when the barrier width begins to approach a value which is twice the width of the interface. The calculated values for both $\bar{x}_b$ and $\bar{x}_w$ are listed in Table 1. The following empirical relationship is the result of a fit of an exponential function to the calculated values of $\bar{x}_b$ and the barrier widths:

$$\bar{x}_b = x_o(2 - e^{(6.4/\bar{t}_b)}) \tag{5}$$

where $\bar{t}_b$ is the barrier width in Å and x_o is the Cd concentration of a very thick barrier, i.e. the Cd concentration of alloys grown under the same conditions.

If this model is correct then the Cd concentration of the barrier at a position at least four monolayers removed from the interface is x_o. Therefore the value of x_o, i.e. 0.68 ± 0.02 together with an interdiffusion width or interface width was used in the band structure calculations discussed below. Obviously the diffusion which has taken place at the interface becomes increasingly more significant with decreasing barrier width.

One of the superlattices, Q250b, with the extremely short period of 31.4 Å was annealed at 250°C for 24 hours under an Hg atmosphere. The x value of the resulting alloy was determined from transmission and reflection measurements to be 0.24 and 0.22, respectively. If all of the CdTe is in the barrier whose width is 20.0 Å then the x value of the barrier is about 0.36. For this narrow well width, i.e. 11.4 Å, however this is not a realistic assumption as suggested by the calculated value for $\bar{x}_w$, i.e. 0.04, which is listed together with values for all of the superlattices in Table 1. Therefore the average x value in the barrier should be somewhat less than 0.36.

Obviously appreciable interdiffusion has taken place in Q250b. The initial barrier composition, $\bar{x}_b$, was 0.68 according to the alloys grown under nearly identical growth conditions. This superlattice consists of 900 periods, each with a width of 31.4 Å, which were subjected to the growth temperature of 180°C for 4 hours. As mentioned above, Kim *et al.*[8] have shown that interdiffusion is larger near the surface. Their published values for the Hg diffusion constant at 180°C are approximately 1×10^{-17}, 1×10^{-18} and 1×10^{-19} cm^2sec^{-1} for the depths of 100, 3500 and 7000 Å respectively. The time spent at a distance of 3500 Å or less from the surface was 30 minutes. Thus to a first approximation, an interdiffusion width for Hg of $2\pi \cdot \sqrt{Dt} \approx 20$ Å can be expected. This is roughly the barrier width

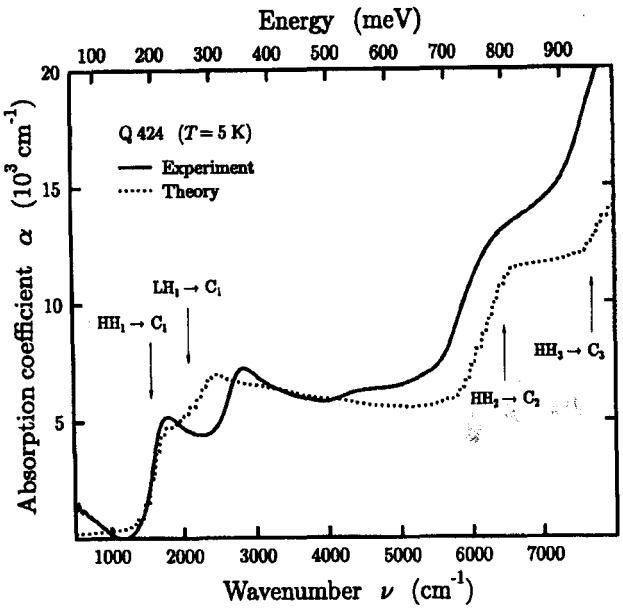

FIG. 7. The experimental and theoretical optical absorption coefficient as a function of wavenumber (cm^{-1}) and energy (eV) for the superlattice Q424 at 5 K. Theoretically determined values of various subband transitions are indicated, e.g. $HH_1 \rightarrow C_1$.

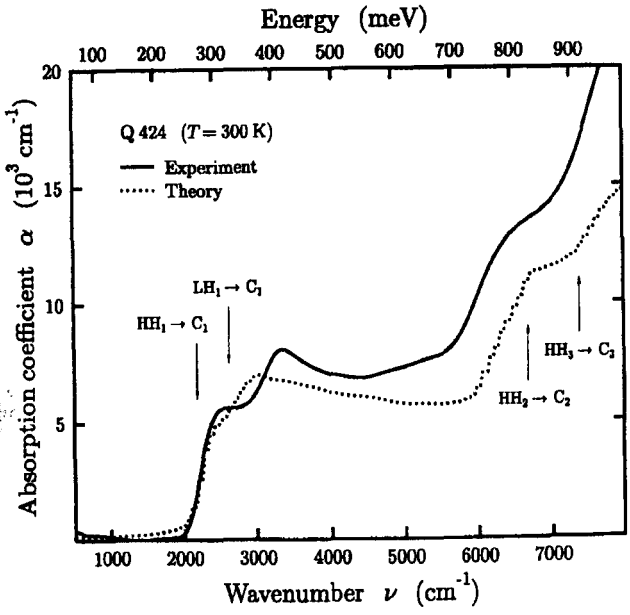

FIG. 8. The experimental and theoretical optical absorption coefficient as a function of wavenumber (cm^{-1}) and energy (eV) for the superlattice Q424 at 300 K. Theoretically determined values of various subband transitions are indicated, e.g. $HH_1 \rightarrow C_1$.

and therefore a reduction in the empirical value of $\bar{x}_b$ from 0.68 for a very wide barrier to 0.44 or less for a barrier width of 20.0 Å is reasonable. The experimental value for $\bar{x}_b$ of 0.36 ± 0.05 is smaller than the empirical value. Apparently less Cd is incorporated into very narrow barriers. This is corroborated by the theoretical predictions discussed in the next section concerning the maximum Cd concentration, i.e. $x_o = 0.40$ for Q250, in very narrow barriers which is required for reasonable agreement between experimental and theoretical values of the absorption coefficient.

D. Optical absorption coefficient

The experimentally and theoretically determined optical absorption coefficients for the superlattice Q424 at 5 and 300 K are shown in Fig.7 and Fig.8, respectively. Theoretically determined energies of various transitions, which are indicated by arrows, correspond to the observed structure in the absorption coefficient. The energy of the transition from the first heavy hole subband to the first conduction subband ($HH_1 \rightarrow C_1$) transition decreases from 272 to 180 meV when the temperature is lowered from 300 to 5 K. The theoretical value for the ($HH_1 \rightarrow C_1$) transition is 84 ± 6 meV lower at 5 K and 64 ± 6 meV lower at 77 K for all of the superlattices with the exception of the three with extremely narrow well or barrier widths, i.e. Q250, Q211 and Q178. The temperature dependence of the transition from the first light hole subband to the first conduction subband ($LH_1 \rightarrow C_1$) is somewhat smaller and that of the higher order transitions, e.g. $HH_2 \rightarrow C_2$, is less regular. These statements concerning the relative temperature dependence of the subband transitions are true for all of the investigated superlattices with the exception stated above. The step in the absorption coefficient between 800 and 900 meV, which is due to $HH_2 \rightarrow C_2$ and $HH_3 \rightarrow C_3$ in this case, is nearly temperature independent.

A comparison of the experimentally and theoretically determined absorption coefficients is made in Fig.9 for the superlattice Q426 at 300 K. The fit for Q426 as well as for Q424, which is shown in Figs. 7 and 8, is excellent with two exceptions, when one considers the fact that no adjustable parameters were used in the theoretical calculations. The first exception is the discrepency in the minor structure due to the $LH_1 \rightarrow C_1$ transition which is sometimes refered to as the interface subband to conduction subband ($I_1 \rightarrow C_1$) transition. This discrepency is not understood at the present time. One possible cause of the shift of the experimental peak to higher energies is the Burstein-Moss

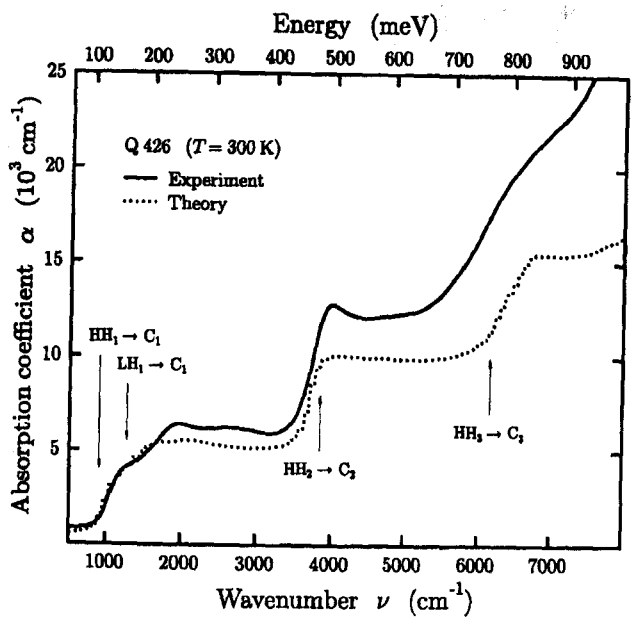

FIG. 9. The experimental and theoretical optical absorption coefficient as a function of wavenumber (cm^{-1}) and energy (eV) for the superlattice Q426 at 300 K. Theoretically determined values of various subband transitions are indicated, e.g. $HH_1 \rightarrow C_1$.

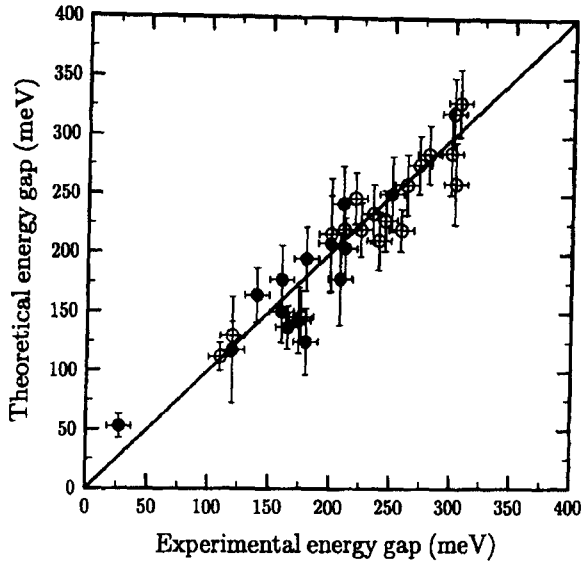

FIG. 10. Experimental and theoretical values of the energy gap, i.e. $HH_1 \rightarrow C_1$. Values for 300 K are indicated by empty circles and those for 5 K by filled circles. The error bars for the theoretically determined energy gap correspond to the experimental uncertainity in the well and barrier thicknesses, i.e. ±3 Å or about one monolayer.

shift due to filling of either the conduction or valence subband. However according to our calculations, a shift of the Fermi energy from the valence band HH_1 to the conduction band C_1 for Q424, which corresponds to a carrier concentration of $\geq 2 \times 10^{17}$, can not account for this discrepency. The second exception is the difference in magnitude of the absorption coefficient at higher energies which is only partially due to an increased experimental uncertainity in the absorption coefficient for larger absorption coefficients.

Experimental and theoretical values for the energy gap, i.e the $HH_1 \rightarrow C_1$ transition for these superlattices, are listed in Table 1 and shown in Fig.10. The energy of the $HH_1 \rightarrow C_1$ transition depends on the period, the well thickness and on the x_o value of the barrier in a complicated manner. However the structure in the absorption coefficient between 800 and 900 meV depends only on the x_o value of the barrier. The energy and the shape of this structure in the absorption coefficient is only in good agreement with theory if the x_o value of the barrier is taken to be 0.68 ± 0.02, with the following exception.

Theoretical values for the energy gap and the absorption coefficient for the superlattices with extremely narrow well or barrier widths, i.e. Q250, Q211 and Q178, were in satisfactory agreement with experiment, only if the x_o value of the barrier was assumed to be less than 0.68 ± 0.02, e.g. 0.40 for Q250. Apparently there is less Cd in very narrow barriers than expected if the Cd concentration profile as determined by Kim *et al.*[8] is assumed to be applicable for these barriers.

IV. CONCLUSIONS

Both the well width as well as the period of a number of MBE grown short period (001) $Hg_{1-x}Cd_xTe$-HgTe superlattices were determined directly by x-ray diffraction. The well width was determined by exploiting the high reflectivity from HgTe and the low reflectivity from CdTe for the (002) Bragg reflection. An upper limit for the average composition of the barriers, $\bar{x}_b$, was determined for the barriers. $\bar{x}_b$ was found to decrease exponentially with decreasing barrier width, *e.g.* $\bar{x}_b \approx 0.64$ and 0.36 for barrier widths of 90.7 and 20.0 Å respectively. This exponential dependence can be explained by assuming that the width and shape of the $Hg_{1-x}Cd_xTe$/HgTe interface

of all the investigated superlattices are identical to an experimentally determined concentration profile.[8] The relative importance of this interface, i.e. interdiffusion between the barrier and well, increases with deceasing barrier width.

The experimentally determined energy gap at 5 and 300 K for all the investigated superlattices with only several exceptions are in good agreement with theoretical predictions. As mentioned above, this theory does not contain any adjustable parameters. This statement concerning good agreement between experiment and theory is also true for the absorption coefficient. The energy gap which is due to the $HH_1 \rightarrow C_1$ transition for these superlattices depends on the period, the well thickness and on the x_o value of the barrier in a complicated manner. However the structure in the absorption coefficient between 800 and 900 meV depends only on the x_o value of the barrier. The energy and the shape of this structure in the absorption coefficient is only in good agreement with theory if the x_o value of the barrier is taken to be 0.68 ± 0.02 with the exception of superlattices with extremely narrow wells or barriers.

ACKNOWLEDGMENTS

The support of this project by the Bundesministerium für Forschung und Technologie (contract number TK 0369), the Deutsche Forschungsgemeinschaft and the Alexander von Humboldt-Stiftung is gratefully acknowledged.

---

[a] Permanent Address: Shanghai Institute of Technical Physics, Chinese Academy of Sciences, Shanghai, People's Republic of China

[1] J.N.Schulman, and T.C.McGill, Appl. Phys. Lett. **34**, 663 (1979).
[2] J.P.Faurie, A.Million and J.Piaguet, Appl. Phys. Lett. **41**, 713 (1982).
[3] J.P.Faurie, IEEE J. Quantum Electron. **QE-22**, 1656 (1986).
[4] T.C.McGill, G.Y.Wu and S.R.Hetzler, J. Vac. Sci. Technol. A **4**, 2091 (1986).
[5] J.R.Meyer, C.A.Hoffman and F.J.Bartoli, Semicond. Sci. Technol. **5**, S90 (1990) and references therein.
[6] D.L. Smith, T.C.McGill and J.N. Schulman, Appl. Phys. Lett. **43**, 180 (1983).
[7] J. Reno and J.P. Faurie, Appl. Phys. Lett. **49**, 409 (1986).
[8] Y.Kim, A.Ourmazd, M.Bode and R.D.Feldman, Phys. Rev. Lett. **63**, 636 (1989).
[9] J.N.Schulman, O.K.Wu, E.A.Patten, J.W.Han, Y.Lansari, L.S.Kim, J.W.Cook, Jr. and J.F.Schetzina, Appl. Phys. Lett. **53**, 2420 (1988).
[10] M. Möller, R.N. Bicknell-Tassius and G. Landwehr, J. Appl. Phys. **72**, 5108 (1992).
[11] C.R. Becker, L. He, M.M. Regnet, M.M. Kraus, Y.S. Wu, G. Landwehr, X.F. Zhang and H. Zhang, to be published in J. Appl. Phys., Aug. (1993).
[12] L.R. Ram-Moham, K.H. Yoo and R.L. Aggarwal, Phys. Rev. B **38**, 6151 (1988).
[13] N.F. Johnson, H. Ehrenreich, P.M. Hui and P.M. Young, Phys. Rev. B **41**, 3655 (1990).
[14] A. Simon, D. Bertho, D. Boiron and C. Jonanin, Phys. Rev. B **42**, 5221 (1990).
[15] E. Bangert, P. Boege, V. Latussek and G. Landwehr, Semicond. Sci. Technol. **8**, S99 (1993).
[16] Y.S.Wu, C.R.Becker, A.Waag, R.N.Bicknell-Tassius and G. Landwehr, Appl. Phys. Lett. **60**, 1878 (1992).
[17] Y.S. Wu, C.R. Becker, A. Waag, R. Schmiedl, S. Einfeldt and G. Landwehr, J. Appl. Phys. **73**, ... (1993).
[18] Y.S.Wu, C.R.Becker, A.Waag, R.N.Bicknell-Tassius and G. Landwehr, J. Appl. Phys. **69**, 268 (1991).
[19] M.Quillec. *Structural Characterization of Superlattices by x-Ray diffraction.*, Springer Proceedings in Physics (Les Houches, France, 1986), Vol. 13, pp. 121 ff.
[20] G.L. Hansen, J.L. Schmit and T.N. Casselman, J. Appl. Phys. **53**, 7099 (1982).
[21] R.R. Galazka and A. Kisiel, Phys. stat. sol. **34**, 63 (1969).
[22] L. He, C.R Becker, R.N. Bicknell-Tassius, S. Scholl and G. Landwehr, J. Appl. Phys. **73**, 3305 (1993).
[23] M.H. Weiler, *Semiconductors and Semimetals*, Vol. 16, editors R. Willardson and A.C. Beer, Academic Press, New York, pp. 119, 1981.
[24] C.K. Shih and W.E. Spicer, Phys. Rev. Lett. **58**, 2594 (1987).
[25] M.M. Kraus, M.M. Regnet, C.R. Becker, R.N. Bicknell-Tassius and G. Landwehr, J. Appl. Phys. **71**, 5610 (1992).
[26] T.H. Myers, R.W. Yanka, K.A. Harris, A.R. Reisinger, J. Han, S. Hwang, Z. Yang, N.C. Giles, J.W. Cook Jr., J.F.Schetzina, R.W. Green and S. McDevitt, J. Vac. Sci. Technol. A **7**, 300 (1989).
[27] J.Reno, R.Sporken, Y.J.Kim, C.Hsu and J.P.Faurie, Appl. Phys. Lett. **51**, 1545 (1987).
[28] E. Monterrat, L. Ulmer, R.Mallard, N.Magnea and J.L. Pautrat, J. Appl. Phys. **73**, 1774 (1992).